



Cite this: *New J. Chem.*, 2021, **45**, 4414

Received 25th January 2021,
Accepted 12th February 2021

DOI: 10.1039/d1nj00388g

rsc.li/njc

Hydrazone exchange: a viable route for the solid-tethered synthesis of [2]rotaxanes†

Rafael Da Silva Rodrigues,^a Ena T. Luis,^{id}^{ab} David L. Marshall,^{id}^{bc}
John C. McMurtrie^{id}^{ab} and Kathleen M. Mullen^{id}^{*ab}

Controlled and complete assembly of supramolecular systems on solid supports is a challenge that would elevate the function of interlocked architectures. Building on the success of other dynamic covalent synthetic methods, we present hydrazone exchange as a strategy to improve the formation of rotaxanes in solution and on solid surfaces. Solution-state analogues containing naphthalenediimide (NDI) or bipyridinium motifs and 1,5-dinaphtho[38]crown-10 were initially prepared to establish ideal conditions for maintaining thermal equilibrium throughout the exchange reaction. Solid-state rotaxanes were synthesised on hydrazide-functionalised TentaGel™ polymer resins and analysed with HR MAS ¹H NMR spectroscopy. Surface rotaxane functionalisation of 80% was achieved for the NDI rotaxane, which is significantly higher than previously reported with either dynamic covalent or traditional irreversible synthetic strategies.

Introduction

Interlocked architectures such as rotaxanes and catenanes have shown great promise as components in molecular machines.^{1–6} In recent years, they have been developed for applications across catalysis,^{7–12} sensing,^{13–16} drug delivery,^{17–19} nano-electronics,^{20–22} *in vivo* imaging^{23–26} and the development of stimuli-responsive materials.^{27–29} The majority of known interlocked architectures have shown impressive capabilities in solution; however, incorporation of these components onto solid supports and surfaces opens new possibilities for their functionality.^{30–38} By organising functional rotaxanes into an ordered array, their unique properties can be directed towards a controlled macroscopic output.^{39–41} The generation and characterisation of functionalised solids with little contamination from unwanted by-products has thus been the focus of intense research.^{42–48} Understanding the role of surface attachment on modulating molecular motion in surface-bound bistable rotaxanes and catenanes is of fundamental importance, with some studies revealing significant differences in the way supramolecular switches function when embedded in solids or attached to surfaces.^{49–51}

One challenge with incorporating these structures on surfaces is ensuring the high ratio of interlocked to non-interlocked components at the solution–surface interface. In the solution state, dynamic covalent chemistry has proven to be an attractive synthetic strategy for the preparation of interlocked architectures and molecular machines.^{52–60} The reversibility of this class of reactions introduces a proofreading step into the reaction mechanism,^{61,62} which maximises the proportion of interlocked components at the expense of non-interlocked by-products that are typically kinetically favoured. Pioneering work by Sanders and co-workers^{63–66} demonstrated the successful synthesis of a number of catenanes using dynamic reactions initially focused on disulfide exchange. Their work demonstrates that control of the library can be easily manipulated through careful design and a detailed understanding of constitutional, steric, and electronic effects to amplify the desired product.^{67–69} These fundamental studies ultimately led to the synthesis of a macromolecular trefoil knot in near quantitative yield.⁷⁰

Dynamic covalent chemistry is also an effective strategy for rotaxane formation in the gel phase. We have recently reported^{71,72} the successful functionalisation of TentaGel™ polymer resins with [2]rotaxanes using a synthetic approach involving dynamic disulfide exchange. Conventional irreversible synthetic strategies typically led to a low proportion of the desired rotaxanes (20–40%)⁷³ compared to non-interlocked components, complicating the characterisation and rendering the solid supports non-homogeneous and therefore inherently less useful. The reversibility offered by the incorporation of disulfide exchange in the resin functionalisation step led to an improvement in surface homogeneity, with up to 60% coverage of the polymer resin with

^a School of Chemistry and Physics, Queensland University of Technology, Brisbane, Australia. E-mail: kathleen.mullen@qut.edu.au

^b Centre for Materials Science, Queensland University of Technology, Brisbane, Australia

^c Central Analytical Research Facility, Queensland University of Technology, Brisbane, Australia

† Electronic supplementary information (ESI) available. See DOI: 10.1039/d1nj00388g

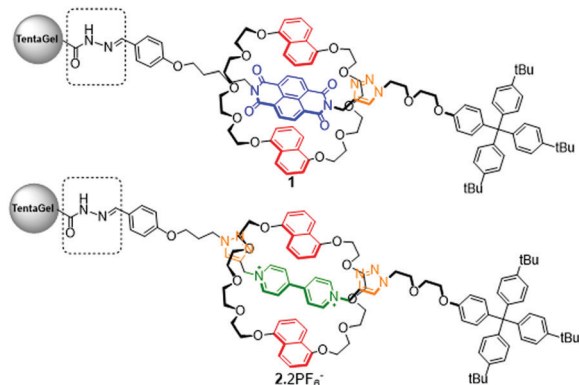


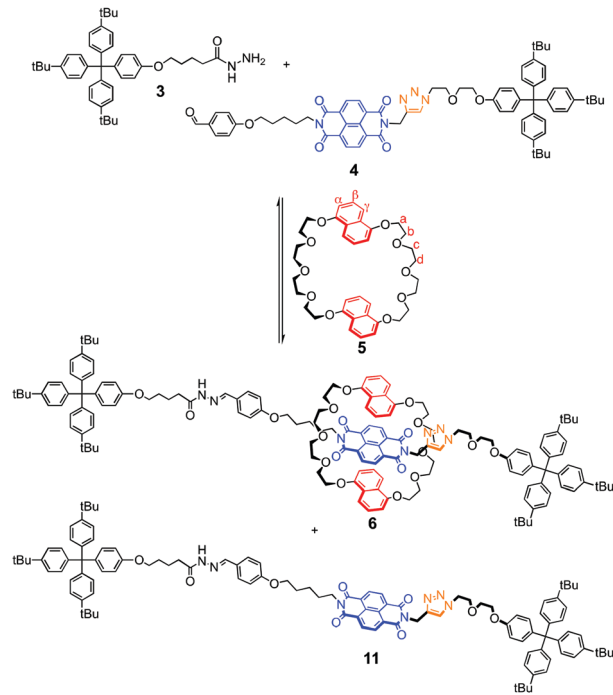
Fig. 1 Target solid-bound [2]rotaxanes synthesised using a hydrazone exchange methodology from hydrazide-functionalised solid supports.

rotaxane. Given the symmetrical nature of the disulfide reaction mechanism, however, analysis of the equilibrium was challenging with eight different homo- and heterodimeric dumbbell and rotaxane species present in solution. Whilst it can be argued that rotaxanes could be preformed and then subsequently attached to surfaces, the added benefit of a dynamic covalent approach is that the surfaces could be “reused”, given the reversibility of this surface functionalization. Herein we report the use of dynamic hydrazone exchange^{74,75} to assemble interlocked architectures on polymer resins with the same efficiency as observed in solution, thereby creating functionalised surfaces with limited kinetic by-products that result from traditional approaches. Fig. 1 shows the structures of the target functionalised resins that incorporate 1,5-dinaphtho[38]crown-10 (5) as the macrocycle and a naphthalene diimide^{76–78} (1) or bipyridinium^{79,80} (2) recognition site on the axle. The asymmetrical nature of the hydrazone exchange reaction simplifies the exchange process compared to the disulfide mechanism, and the reaction allows for the incorporation of recognition sites that are unstable under the basic conditions used in disulfide exchange, namely bipyridinium motifs. The stronger interaction between the bipyridinium and crown ether macrocycles,⁸¹ compared to the naphthalene diimide, is expected to further improve the proportion of interlocked architectures attached to the bead.

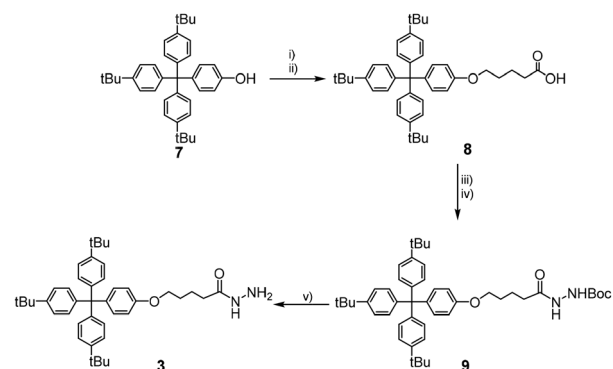
Results and discussion

Synthesis of rotaxanes *via* hydrazone exchange in solution

Our initial efforts focused on the synthesis of naphthalene diimide (NDI) [2]rotaxane **6** (Scheme 1). This necessitated the synthesis of the hydrazide stopper **3** (Scheme 2) and the naphthalene diimide **4** which possesses a terminal aldehyde (Scheme 3). Williamson etherification of phenol stopper **7** with ethyl 5-bromovalerate, followed by hydrolysis of the resulting ester with sodium hydroxide, produced the acid-functionalised stopper **8** in 98% yield (Scheme 2).⁸² Reaction of **8** with thionyl chloride produced the acid chloride derivative which was immediately reacted with *tert*-butyl carbazate to afford the desired Boc-protected hydrazide **9** in 32% yield. Deprotection of **9** was readily achieved by reaction with trifluoroacetic acid



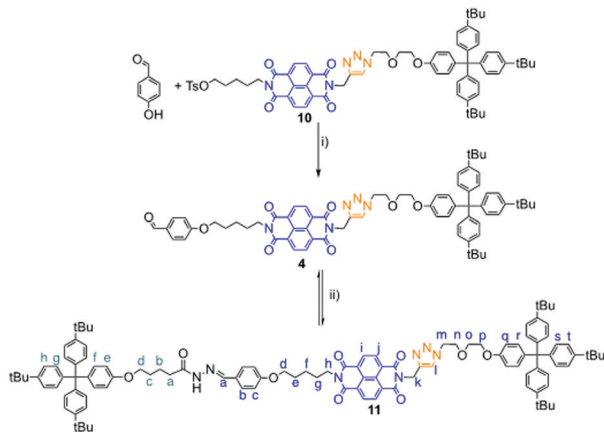
Scheme 1 Synthesis of the solution model hydrazone rotaxane **6** and NDI dumbbell **11**. Reagents and conditions: 1,5-dinaphtho[38]crown-10 macrocycle **5** (5 equiv.), TFA (cat.), r.t., CHCl₃, 7 days.



Scheme 2 Synthesis of hydrazide stopper **3**. Reagents and conditions: (i) ethyl 5-bromovalerate, K₂CO₃, Cs₂CO₃, MeCN, reflux, 3 days, 98%; (ii) CH₂Cl₂/MeOH, NaOH, r.t., 1 h, 99%; (iii) SOCl₂, toluene, reflux, 12 h, quant. yield; (iv) NH₂NHBoc, CH₂Cl₂, 2 days, 32%; (v) CH₂Cl₂/TFA (50%), 45 min, r.t., 90%.

(TFA) to produce the desired hydrazide **3** in 90% yield. The synthesis of the stopper hydrazide was confirmed by ¹H NMR spectroscopy and supported by mass spectrometry (Fig. S1 and S2, ESI[†]). Importantly, the hydrazide stopper **3** was found to be prone to dimerisation at room temperature over time, forming an unreactive dimer **S1**. Thus, for all future exchange reactions, the stopper **3** was deprotected immediately before use.

To obtain aldehyde-functionalised naphthalene diimide thread **4**, NDI tosylate half-dumbbell **10**⁷² was reacted with *p*-hydroxybenzaldehyde, to give the product in 93% yield (Scheme 3). Conditions for the reaction of aldehyde **4** with



Scheme 3 Synthesis of naphthalene diimide dumbbell **11**. Reagents and conditions: (i) K_2CO_3 , Cs_2CO_3 , MeCN, reflux, 3 days, 93%, (ii) **5**, 5 mM, TFA (cat.), CHCl_3 ; yields reported in Table 1.

hydrazide stopper **3** were then screened to better understand the hydrazone equilibrium and optimise the synthesis of both the NDI dumbbell **11** and the desired [2]rotaxane **6** (Scheme 1).

To this end, five small-scale reaction conditions were first trialled probing the effect of the concentration of acid catalyst on the reaction of hydrazide stopper **3** and NDI aldehyde **4**. The reactions were followed for four weeks⁸³ by HPLC equipped with dual mass-spectrometry and UV detection, during which equilibrium was reached and maintained (Table 1 and Fig. S4, ESI[†]). The reaction with no TFA showed minimal formation of the hydrazone dumbbell **11** after four days which remained very low over two weeks (Table 1). All other reactions showed the formation of the desired dumbbell in 65–70% conversion.

The reversibility of the hydrazone exchange reaction is central to the strategy of dynamic rotaxane synthesis. To investigate the reversibility, one equivalent of 1,5-dinaphtho[38]crown-10 macrocycle **5** was added to a pre-equilibrated solution of NDI dumbbell **11** (obtained from reacting hydrazide stopper **3** and NDI aldehyde

4 for four days). The reaction was carried out with different acid catalyst concentrations and the product distributions were monitored (Table 1 and Fig. S5, ESI[†]). Following the addition of macrocycle **5**, a decrease in concentration of dumbbell **11** was observed in conjunction with the appearance of a new chromatographic peak with a retention time of 11.6 min, with a mass corresponding to the [2]rotaxane **6** (m/z 2349.2587, $[\text{M} + \text{H}]^+$). This concomitant decrease in the proportion of dumbbell **11** with the appearance of [2]rotaxane **6** demonstrates that the formation of interlocked structures is only possible due to the reversibility of the hydrazone exchange.

The addition of 5 equivalents of macrocycle **5** resulted in conversions of up to 42% of the desired [2]rotaxane **6** (Fig. S6 and Table S5, ESI[†]). Solutions with higher concentrations of acid catalyst (0.1% and 0.5%) were able to re-equilibrate more rapidly to produce rotaxane **6** in reasonable conversion (~28%) after only three days. In order to balance the time necessary to reach thermodynamic equilibrium whilst keeping the acid concentrations as low as possible, the ideal condition chosen moving forward was 0.1% TFA in chloroform with the concentration of hydrazide and aldehyde at 5 mM.

Using these conditions, the synthesis of dumbbell **11** and [2]rotaxane **6** were then carried out on a preparative scale. To this end, 5 equivalents of macrocycle **5** (25 mM) and TFA (0.1%) were added to a 5 mM solution of hydrazide stopper **3** and NDI aldehyde **4**. After 7 days, the reaction was quenched (by addition of $\text{Na}_2\text{CO}_3(\text{aq})$) and, following column chromatography, the desired [2]rotaxane **6** was obtained as a red solid in 35% yield. The red colouration is a result of charge transfer interactions between the electron-rich macrocycle and electron-deficient naphthalene diimide, and is indicative of a mechanically interlocked topology⁷³ (Fig. S7, ESI[†]). Dumbbell **11** was also isolated from the reaction mixture in 52% yield. The partial ¹H NMR spectra of dumbbell **11** and [2]rotaxane **6** in CDCl_3 are displayed in Fig. 2. For the rotaxane **6**, significant upfield shifts in signals for the naphthalene diimide protons H_i and H_j ($\Delta\delta = 0.46$ ppm), and macrocycle aromatic protons H_α , H_β and H_γ ($\Delta\delta_\alpha = 0.53$ ppm, $\Delta\delta_\beta = 0.76$ ppm, and $\Delta\delta_\gamma = 0.98$ ppm) were observed due to π - π stacking interactions between the crown ether macrocycle and naphthalene diimide thread, indicative of successful rotaxane formation. Additional proof of the rotaxane formation is shown by the short distance cross-peaks between signals H_i and H_j of the NDI centre and signals H_γ , H_α , H_β , H_c and H_d of the macrocycle observed in the 2D-ROESY NMR spectrum (Fig. S8, ESI[†]).

To examine the versatility of hydrazone exchange to other supramolecular motifs, attention was turned towards the synthesis of bipyridinium rotaxane **17.2PF₆⁻**. The synthesis of aldehyde functionalised bipyridinium thread **15.2PF₆⁻** was achieved as outlined in Scheme 4. Reaction of 4-(3-hydroxypropoxy)benzaldehyde **12** with tosyl chloride in the presence of triethylamine afforded 3-(4-formylphenoxy)propyl toluenesulfonate as a colourless solid in 66% yield. This was then reacted with sodium azide to give **13** in 96% yield. Coupling of the alkyne-functionalised mono-stoppered bipyridinium thread **14.2PF₆⁻** with azide **13** via a copper(i) catalysed alkyne-azide cycloaddition (CuAAC) reaction afforded

Table 1 Monitoring the hydrazone exchange between NDI aldehyde **4** and hydrazide stopper **3**, in the absence and presence of macrocycle **5**, as a function of acid catalyst concentration.^a

% TFA	Reaction without macrocycle 5		Reaction with 1 equiv. macrocycle 5 ^b		
	% NDI aldehyde 4 (4.7 min)	% NDI dumbbell 11 (11.1 min)	% NDI aldehyde 4 (4.7 min)	% NDI dumbbell 11 (11.1 min)	% NDI rotaxane 6 (11.6 min)
0	>99	<1	90	10	0
0.001	30	70	32	56	12
0.01	31	69	38	39	24
0.1	30	70	38	31	32
0.5	35	65	39	35	26

^a Normalised peak areas of aldehyde **4**, dumbbell **11** and rotaxane **6** after 7 days as determined by HPLC at $\lambda = 380$ nm are reported. NDI-containing products were detected at this wavelength; hydrazide stopper **3** was not detected and is excluded from this comparison. The data compares the proportions of aldehyde, dumbbell and rotaxane after each reaction. ^b Numbers may not add to 100% due to rounding.

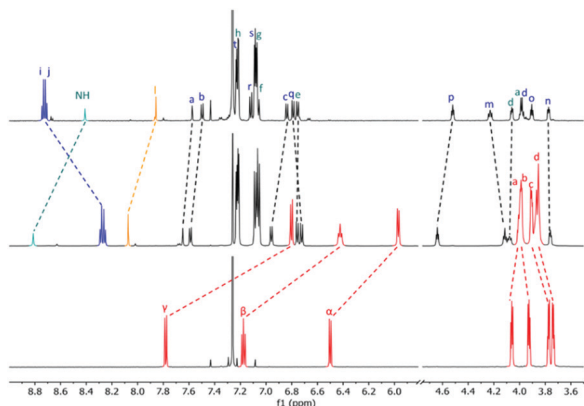


Fig. 2 ^1H NMR (CDCl_3 , 600 MHz) comparison of the NDI dumbbell **11** (top), the corresponding [2]rotaxane **6** (middle) and the 1,5-dinaphtho[38]crown-10 macrocycle **5** (bottom).

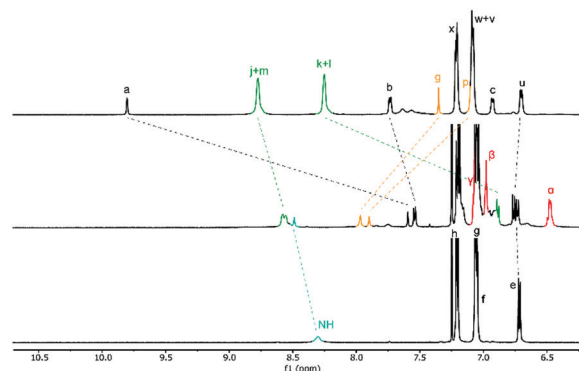
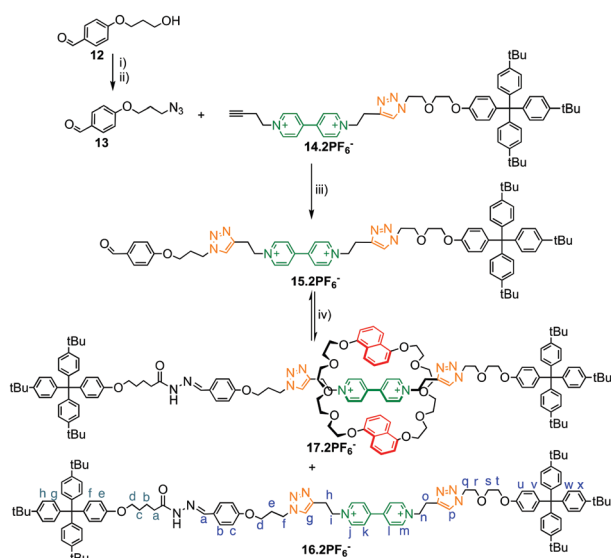


Fig. 3 Partial ^1H NMR spectrum (CDCl_3 , 600 MHz) of the bipyridinium half-dumbbell **15.2PF₆⁻** (top), the hydrazone bipyridinium [2]rotaxane **17.2PF₆⁻** (middle) and the hydrazide stopper **3** (bottom).



Scheme 4 Synthesis of the bipyridinium rotaxane **17.2PF₆⁻**. Reagents and conditions: (i) TsCl, TEA, DMAP, CH_2Cl_2 , $0\text{ }^\circ\text{C} \rightarrow \text{r.t.}$, 66%; (ii) NaN_3 , DMF, $120\text{ }^\circ\text{C}$, 96%; (iii) $[\text{Cu}(\text{CN})_4]\text{PF}_6$, TBTA, CH_2Cl_2 , 58%; (iv) **3**, 5 equiv. macrocycle **5**, 5 mM, TFA (cat.), CHCl_3 , 12% **17.2PF₆⁻**.

the desired bipyridinium half-dumbbell **15.2PF₆⁻** in 58% yield (Fig. S9, ESI[†]).

To investigate the viability of using hydrazone exchange to assemble bipyridinium rotaxanes, the bipyridinium half-dumbbell **15.2PF₆⁻** was reacted with the hydrazide stopper **3** and macrocycle **5** in chloroform with TFA (0.1%) to form the bipyridinium dumbbell **16.2PF₆⁻** and rotaxane **17.2PF₆⁻** (Scheme 4). Attempts to monitor these reactions *via* HPLC were unsuccessful either as a result of broad elution profiles (when using water:acetonitrile or isopropanol:acetonitrile mixtures) or due to decomposition of the mixture (when using water and acetonitrile with 0.1% formic acid, commonly used for the purification of similar bipyridinium-containing molecules). Nevertheless, by using the conditions established for the NDI

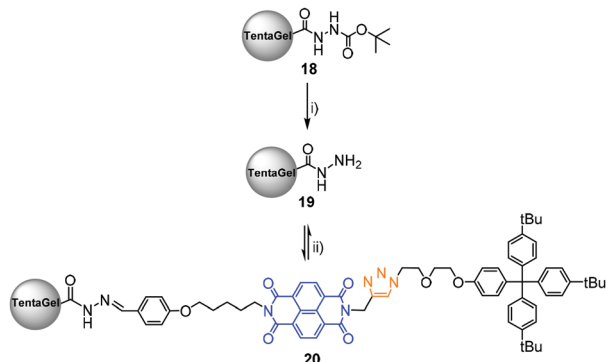
rotaxane **6** described above, the preparative-scale synthesis afforded the desired [2]rotaxane **17.2PF₆⁻** as a red solid in 12% yield. High resolution electrospray ionisation mass spectrometry revealed a peak at $m/z = 1160.6640$ corresponding to the rotaxane **17.2PF₆⁻** ($[\text{M} - 2\text{PF}_6]^{2+}$, Fig. S30, ESI[†]). In addition, large upfield shifts of the signals for the bipyridinium protons $\text{H}_{j/m}$ and $\text{H}_{k/l}$ ($\Delta\delta = 0.19, 1.25$ ppm respectively) and the macrocycle protons H_β and H_γ ($\Delta\delta = 0.10$ ppm and 0.80 ppm respectively) were observed in the ^1H NMR spectrum (Fig. 3). The magnitude of these upfield shifts is consistent with comparable literature reports of bipyridinium based rotaxanes,⁷³ indicating rotaxane formation.⁸⁴

Functionalisation of TentaGel™ resins with hydrazide

Having established ideal conditions for the synthesis of [2]rotaxanes using hydrazone exchange in solution, attention was then turned to the functionalisation of polymer resins using this approach. Unlike surfaces such as glass and gold, the use of these resins allows the collection of solution-like quality ^1H NMR spectra when using a high-resolution magic angle spinning (HR MAS) NMR probe.^{85,86} This technique thus enables a detailed investigation into the binding and dynamic behaviour of these topologically complex materials, which is particularly important when investigating systems that may not have photo- or electroactive reporting groups.

The commercially available Boc-Hydrazido protected resins, TentaGel™-CONHNHBoc **18** were deprotected with 50% TFA/ CHCl_3 for 30 minutes (Fig. S10, ESI[†]). As a proof of concept, hydrazide **19** was reacted with naphthalene diimide thread **4** (5 equiv.) in the presence of 0.1% TFA in chloroform to produce dumbbell functionalised resins **20** (Scheme 5). The HR MAS ^1H NMR spectrum (Fig. 4) shows clear evidence of functionalisation of the resin with the naphthalene diimide thread, with peaks for the NDI moiety observed at 8.71 ppm, and the tetraphenyl stopper group observed at 7.09 and 6.79 ppm.

The reaction was then repeated with five equivalents of macrocycle **5** (relative to **4**) to produce the desired rotaxane-functionalised resins **1**. After two weeks, the reaction was quenched and the resulting red-coloured resins were washed



Scheme 5 Synthesis and functionalisation of Tentagel™ hydrazide resin **19**. Reagents and conditions: (i) TFA/CHCl₃ (50%), 30 min; (ii) **4** (5 equiv.), 5 mM, 0.1% TFA, CHCl₃, 14 days.

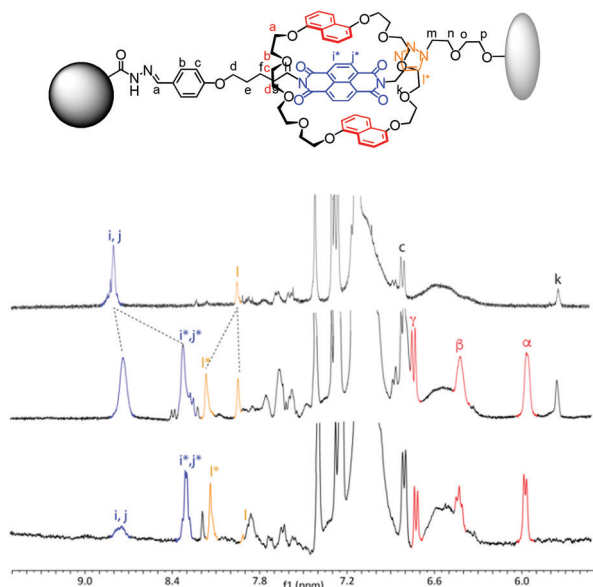


Fig. 4 Partial HR-MAS ¹H NMR (CDCl₃, 400 MHz, 32 CPMG loops) spectra of the resin bound NDI dumbbell **20** (top), rotaxane **1** when the bead functionalisation is performed at room temperature (middle), and rotaxane **1** when the bead functionalisation is performed at $-18\text{ }^{\circ}\text{C}$ (bottom). Comparison of the signals corresponding to $H_{i/j}$ (dumbbell) and H_{i^*/j^*} (rotaxane) shows that rotaxane formation is more favoured at lower temperatures, resulting in 80% functionalisation at $-18\text{ }^{\circ}\text{C}$ compared to 50% functionalisation at room temperature.

extensively to remove any unreacted material.⁸⁷ Successful rotaxane formation on the polymer surface was supported by HR MAS ¹H NMR data (Fig. 4). Two sets of peaks for the diimide protons (H_i and H_j) are observed, with those corresponding to the non-interlocked thread observed at 8.62 ppm, while those indicative of rotaxane formation appear upfield at 8.24 ppm. Likewise, peaks for the crown ether macrocycle protons (H_x , H_β and H_r) were observed at 6.77 ppm, 6.40 and 5.95 ppm, respectively. These chemical shifts are comparable to those observed in the corresponding solution-state rotaxane **6**. Integration of the 1D HR MAS spectrum before application of the

CPMG pulse sequence indicates that the target naphthalene diimide rotaxane species **1** accounted for approximately 50% of the total bead tethered population with the remaining surface covered by the non-interlocked thread, a significant improvement on literature reports using irreversible coupling methods (typically $\sim 20\%$).⁷³ The surface functionalisation reaction was then repeated at $-18\text{ }^{\circ}\text{C}$. At lower temperatures, the interaction between the half-dumbbell and the macrocycle is amplified,^{88,89} which in turn should favour the formation of interlocked species. Again, two sets of peaks corresponding to the dumbbell and rotaxanes are observed in the HR MAS ¹H NMR spectrum (Fig. 4). However, integration of the 1D NMR spectra shows that the proportion of rotaxane on the resin is $\sim 80\%$, a far higher ratio than ever previously reported.^{51,72}

The functionalisation of the hydrazide beads with bipyridinium based rotaxanes was then investigated (Schemes S1 and S2, ESI†). Hydrazide resin **19** was reacted with bipyridinium aldehyde **15.2PF₆⁻** in the presence of five equivalents of the macrocycle **5** and 0.1% TFA. The analogous dumbbell functionalised resins **21.2PF₆⁻** were also prepared as a control. The resulting HR MAS ¹H NMR spectrum of the dried beads **2.2PF₆⁻** can be seen in Fig. S11 (ESI†). The spectrum shows two sets of signals: H_j , H_k , H_l and H_m for the non-interlocked dumbbell ($\delta = 8.80, 8.47, 8.35$ and 8.10 ppm) and $H_{j^*/m}^*$ and $H_{k^*/l}^*$ for the rotaxane structures at 8.07 ppm and 6.98 ppm. In addition, signals for the naphthyl units of the macrocycle were observed at 6.63, 7.10 and 7.19 ppm, which were comparable with similar rotaxanes attached to polymer resins.⁷³ Unfortunately, given the broad and overlapping rotaxane signals with other signals of the structure, the proportion of rotaxane attached to the resins was not able to be calculated. Although rotaxane formation was observed in both cases, unambiguous characterisation of resin-bound rotaxanes with HR MAS ¹H NMR spectroscopy is more suited to the NDI-functionalised thread compared to the analogous bipyridinium system.

Conclusions

In this work, we have demonstrated that hydrazone exchange can be used for the synthesis of rotaxanes in solution and to pattern polymer resin beads with rotaxanes. This strategy builds on previous success with a disulfide exchange mechanism,⁷² and overcomes its limitation of requiring building blocks resistant to basic conditions. Initial investigations both demonstrate that the presence of an acid catalyst is required for dynamic exchange to take place in any appreciable timeframe, and prove that the equilibrium is under thermodynamic control.

Using this reversible approach, a high proportion of the NDI rotaxane was obtained in solution, with surface functionalisation of up to 80% achieved for this system. This yield is significantly higher than that typically achieved by traditional synthetic approaches as well as other dynamic exchange methods. As observed in previous studies, the characterisation of resins functionalised with bipyridinium based rotaxanes is challenging due to broad and poorly defined peaks observed in the HR MAS

^1H NMR spectrum. In this example, the stability of the bipyridinium rotaxane may be a factor given the low yields observed for solution analogues, however future work optimising the HR MAS pulse sequences is needed to improve the characterisation of resins functionalised with charged supramolecular motifs. Nevertheless, this work clearly demonstrates that hydrazone exchange is an effective strategy for the attachment of interlocked architectures onto solid supports. These model components now pave the way for the complete and controlled surface assembly of more complex molecular machines.

Conflicts of interest

There are no conflicts to declare.

Acknowledgements

This work was enabled by use of the Central Analytical Research Facility hosted by the Institute for Future Environments at QUT. Access to CARF is supported by funding from the Faculty of Science, QUT. We also thank the Centre for Materials Science at QUT for funding the postdoctoral fellowship supporting E. T. Luis.

Notes and references

- V. Balzani, M. Gómez-López and J. F. Stoddart, *Acc. Chem. Res.*, 1998, **31**, 405–414.
- J.-P. Sauvage, *Acc. Chem. Res.*, 1998, **31**, 611–619.
- V. Balzani, A. Credi, F. M. Raymo and J. F. Stoddart, *Angew. Chem., Int. Ed.*, 2000, **39**, 3348–3391.
- J.-P. Collin, C. Dietrich-Buchecker, P. Gaviña, M. C. Jimenez-Molero and J.-P. Sauvage, *Acc. Chem. Res.*, 2001, **34**, 477–487.
- E. R. Kay, D. A. Leigh and F. Zerbetto, *Angew. Chem., Int. Ed.*, 2007, **46**, 72–191.
- W. Yang, Y. Li, H. Liu, L. Chi and Y. Li, *Small*, 2012, **8**, 504–516.
- G. De, Bo, S. Kuschel, D. A. Leigh, B. Lewandowski, M. Pappmeyer and J. W. Ward, *J. Am. Chem. Soc.*, 2014, **136**, 5811–5814.
- D. A. Leigh, V. Marcos and M. R. Wilson, *ACS Catal.*, 2014, **4**, 4490–4497.
- J. Beswick, V. Blanco, G. De Bo, D. A. Leigh, U. Lewandowska, B. Lewandowski and K. Mishiro, *Chem. Sci.*, 2015, **6**, 140–143.
- K. Eichstaedt, J. Jaramillo-Garcia, D. A. Leigh, V. Marcos, S. Pisano and T. A. Singleton, *J. Am. Chem. Soc.*, 2017, **139**, 9376–9381.
- L. van Dijk, M. J. Tilby, R. Szpera, O. A. Smith, H. A. P. Bunce and S. P. Fletcher, *Nat. Rev. Chem.*, 2018, **2**, 0117.
- C. Biagini, S. D. P. Fielden, D. A. Leigh, F. Schaufelberger, S. Di-Stefano and D. Thomas, *Angew. Chem., Int. Ed.*, 2019, **58**, 9876–9880.
- S.-Y. Hsueh, C.-C. Lai and S.-H. Chiu, *Chem. – Eur. J.*, 2010, **16**, 2997–3000.
- R. Mitra, M. Thiele, F. Octa-Smolín, M. C. Letzel and J. Niemeyer, *Chem. Commun.*, 2016, **52**, 5977–5980.
- J. Y. C. Lim, I. Marques, V. Félix and P. D. Beer, *J. Am. Chem. Soc.*, 2017, **139**, 12228–12239.
- S. Corra, C. de Vet, J. Groppi, M. La Rosa, S. Silvi, M. Baroncini and A. Credi, *J. Am. Chem. Soc.*, 2019, **141**, 9129–9133.
- H. Yan, C. Teh, S. Sreejith, L. Zhu, A. Kwok, W. Fang, X. Ma, K. T. Nguyen, V. Korzh and Y. Zhao, *Angew. Chem., Int. Ed.*, 2012, **51**, 8373–8377.
- R. Barat, T. Legigan, I. Tranoy-Opalinski, B. Renoux, E. Péraudeau, J. Clarhaut, P. Poinot, A. E. Fernandes, V. Aucagne, D. A. Leigh and S. Papot, *Chem. Sci.*, 2015, **6**, 2608–2613.
- G. Yu, D. Wu, Y. Li, Z. Zhang, L. Shao, J. Zhou, Q. Hu, G. Tang and F. Huang, *Chem. Sci.*, 2016, **7**, 3017–3024.
- J. E. Green, J. Wook Choi, A. Boukai, Y. Bunimovich, E. Johnston-Halperin, E. DeIonno, Y. Luo, B. A. Sheriff, K. Xu, Y. Shik Shin, H.-R. Tseng, J. F. Stoddart and J. R. Heath, *Nature*, 2007, **445**, 414–417.
- A.-J. Avestro, D. M. Gardner, N. A. Vermeulen, E. A. Wilson, S. T. Schneebeli, A. C. Whalley, M. E. Belowich, R. Carmieli, M. R. Wasielewski and J. F. Stoddart, *Angew. Chem., Int. Ed.*, 2014, **53**, 4442–4449.
- H. Masai, J. Terao, S. Seki, S. Nakashima, M. Kiguchi, K. Okoshi, T. Fujihara and Y. Tsuji, *J. Am. Chem. Soc.*, 2014, **136**, 1742–1745.
- J. R. Johnson, N. Fu, E. Arunkumar, W. M. Leevy, S. T. Gammon, D. Piwnica-Worms and B. D. Smith, *Angew. Chem., Int. Ed.*, 2007, **46**, 5528–5531.
- J.-J. Lee, A. G. White, J. M. Baumes and B. D. Smith, *Chem. Commun.*, 2010, **46**, 1068–1069.
- S. Guha, G. K. Shaw, T. M. Mitcham, R. R. Bouchard and B. D. Smith, *Chem. Commun.*, 2016, **52**, 120–123.
- C. Zhai, C. L. Schreiber, S. Padilla-Coley, A. G. Oliver and B. D. Smith, *Angew. Chem., Int. Ed.*, 2020, **59**, 23740–23747.
- J. Berná, D. A. Leigh, M. Lubomska, S. M. Mendoza, E. M. Pérez, P. Rudolf, G. Teobaldi and F. Zerbetto, *Nat. Mater.*, 2005, **4**, 704–710.
- Y. Sagara, M. Karman, E. Verde-Sesto, K. Matsuo, Y. Kim, N. Tamaoki and C. Weder, *J. Am. Chem. Soc.*, 2018, **140**, 1584–1587.
- Q. Zhang, S.-J. Rao, T. Xie, X. Li, T.-Y. Xu, D.-W. Li, D.-H. Qu, Y.-T. Long and H. Tian, *Chem*, 2018, **4**, 2670–2684.
- B. Long, K. Nikitin and D. Fitzmaurice, *J. Am. Chem. Soc.*, 2003, **125**, 15490–15498.
- M. R. Diehl, D. W. Steuerman, H.-R. Tseng, S. A. Vignon, A. Star, P. C. Celestre, J. F. Stoddart and J. R. Heath, *ChemPhysChem*, 2003, **4**, 1335–1339.
- H.-R. Tseng, D. Wu, N. X. Fang, X. Zhang and J. F. Stoddart, *ChemPhysChem*, 2004, **5**, 111–116.
- F. Cecchet, P. Rudolf, S. Rapino, M. Margotti, F. Paolucci, J. Baggerman, A. M. Brouwer, E. R. Kay, J. K. Y. Wong and D. A. Leigh, *J. Phys. Chem. B*, 2004, **108**, 15192–15199.
- A. H. Flood, A. J. Peters, S. A. Vignon, D. W. Steuerman, H.-R. Tseng, S. Kang, J. R. Heath and J. F. Stoddart, *Chem. – Eur. J.*, 2004, **10**, 6558–6564.

- 35 T. J. Huang, B. Brough, C.-M. Ho, Y. Liu, A. H. Flood, P. A. Bonvallet, H.-R. Tseng, J. F. Stoddart, M. Baller and S. Magonov, *Appl. Phys. Lett.*, 2004, **85**, 5391–5393.
- 36 C. M. Whelan, F. Gatti, D. A. Leigh, S. Rapino, F. Zerbetto and P. Rudolf, *J. Phys. Chem. B*, 2006, **110**, 17076–17081.
- 37 B. K. Juluri, A. S. Kumar, Y. Liu, T. Ye, Y.-W. Yang, A. H. Flood, L. Fang, J. F. Stoddart, P. S. Weiss and T. J. Huang, *ACS Nano*, 2009, **3**, 291–300.
- 38 A. C. Fahrenbach, S. C. Warren, J. T. Incorvati, A.-J. Avestro, J. C. Barnes, J. F. Stoddart and B. A. Grzybowski, *Adv. Mater.*, 2013, **25**, 331–348.
- 39 S. Krause and B. L. Feringa, *Nat. Chem. Rev.*, 2020, **4**, 550–562.
- 40 V. N. Vukotic, K. J. Harris, K. Zhu, R. W. Schurko and S. J. Loeb, *Nat. Chem.*, 2012, 456–460.
- 41 B. H. Wilson, L. M. Abdulla, R. W. Schurko and S. J. Loeb, *Chem. Sci.*, 2021, DOI: 10.1039/D0SC06837C.
- 42 C. P. Collier, J. O. Jeppesen, Y. Luo, J. Perkins, E. W. Wong, J. R. Heath and J. F. Stoddart, *J. Am. Chem. Soc.*, 2001, **123**, 12632–12641.
- 43 S. Chia, J. Cao, J. F. Stoddart and J. I. Zink, *Angew. Chem., Int. Ed.*, 2001, **40**, 2447–2451.
- 44 D. W. Steuerman, H.-R. Tseng, A. J. Peters, A. H. Flood, J. O. Jeppesen, K. A. Nielsen, J. F. Stoddart and J. R. Heath, *Angew. Chem., Int. Ed.*, 2004, **43**, 6486–6491.
- 45 K. Nørgaard, B. W. Laursen, S. Nygaard, K. Kjaer, H.-R. Tseng, A. H. Flood, J. F. Stoddart and T. Bjørnholm, *Angew. Chem., Int. Ed.*, 2005, **44**, 7035–7039.
- 46 S. S. Jang, Y. H. Jang, Y.-H. Kim, W. A. Goddard, J. W. Choi, J. R. Heath, B. W. Laursen, A. H. Flood, J. F. Stoddart, K. Nørgaard and T. Bjørnholm, *J. Am. Chem. Soc.*, 2005, **127**, 14804–14816.
- 47 M. A. Olson, A. B. Braunschweig, L. Fang, T. Ikeda, R. Klajn, A. Trabolsi, P. J. Wesson, D. Benítez, C. A. Mirkin, B. A. Grzybowski and J. F. Stoddart, *Angew. Chem., Int. Ed.*, 2009, **48**, 1792–1797.
- 48 Q. Zhang and D.-H. Qu, *ChemPhysChem*, 2016, **17**, 1759–1768.
- 49 L. Raehm, J.-M. Kern, J.-P. Sauvage, C. Hamann, S. Palacin and J.-P. Bourgoïn, *Chem. – Eur. J.*, 2002, **8**, 2153–2162.
- 50 N. Weber, C. Hamann, J.-M. Kern and J.-P. Sauvage, *Inorg. Chem.*, 2003, **42**, 6780–6792.
- 51 R. Da Silva Rodrigues and K. M. Mullen, *ChemPlusChem*, 2017, **82**, 814–825.
- 52 G. R. L. Cousins, S.-A. Poulsen and J. K. M. Sanders, *Chem. Commun.*, 1999, 1575–1576.
- 53 M. von Delius, E. M. Geertsema and D. A. Leigh, *Nat. Chem.*, 2010, **2**, 96–101.
- 54 S. R. Beeren and J. K. M. Sanders, *Chem. Sci.*, 2011, **2**, 1560–1567.
- 55 M. J. Barrell, A. G. Campaña, M. von Delius, E. M. Geertsema and D. A. Leigh, *Angew. Chem., Int. Ed.*, 2011, **50**, 285–290.
- 56 J. M. Klein, J. K. Clegg, V. Saggiomo, L. Reck, U. Lüning and J. K. M. Sanders, *Dalton Trans.*, 2012, **41**, 3780–3786.
- 57 R.-C. Brachvogel and M. von Delius, *Chem. Sci.*, 2015, **6**, 1399–1403.
- 58 S. Lascano, K.-D. Zhang, R. Wehlauch, K. Gademann, N. Sakai and S. Matile, *Chem. Sci.*, 2016, **7**, 4720–4724.
- 59 O. Shyshov, R.-C. Brachvogel, T. Bachmann, R. Srikantharajah, D. Segets, F. Hampel, R. Puchta and M. von Delius, *Angew. Chem., Int. Ed.*, 2017, **56**, 776–781.
- 60 C.-Y. Wang, G. Wu, T. Jiao, L. Shen, G. Ma, Y. Pan and H. Li, *Chem. Commun.*, 2018, **54**, 5106–5109.
- 61 L. Raehm, D. G. Hamilton and J. K. M. Sanders, *Synlett*, 2002, 1743–1761.
- 62 S. Otto, *J. Mater. Chem.*, 2005, **15**, 3357–3361.
- 63 H. Y. Au-Yeung, G. D. Pantoş and J. K. M. Sanders, *Proc. Natl. Acad. Sci. U. S. A.*, 2009, **106**, 10466.
- 64 H. Y. Au-Yeung, F. B. L. Cougnon, S. Otto, G. D. Pantoş and J. K. M. Sanders, *Chem. Sci.*, 2010, **1**, 567–574.
- 65 H. Y. Au-Yeung, G. D. Pantoş and J. K. M. Sanders, *Angew. Chem., Int. Ed.*, 2010, **49**, 5331–5334.
- 66 F. B. L. Cougnon, H. Y. Au-Yeung, G. D. Pantoş and J. K. M. Sanders, *J. Am. Chem. Soc.*, 2011, **133**, 3198–3207.
- 67 H. Y. Au-Yeung, P. Pengo, G. D. Pantoş, S. Otto and J. K. M. Sanders, *Chem. Commun.*, 2009, 419–421.
- 68 H. Y. Au-Yeung, G. Dan Pantoş and J. K. M. Sanders, *J. Am. Chem. Soc.*, 2009, **131**, 16030–16032.
- 69 H. Y. Au-Yeung, G. D. Pantoş and J. K. M. Sanders, *J. Org. Chem.*, 2011, **76**, 1257–1268.
- 70 N. Ponnuswamy, F. B. L. Cougnon, J. M. Clough, G. D. Pantoş and J. K. M. Sanders, *Science*, 2012, **338**, 783.
- 71 H. Wilson, S. Byrne and K. M. Mullen, *Chem. – Asian J.*, 2015, **10**, 715–721.
- 72 R. Da Silva Rodrigues, D. L. Marshall, J. C. McMurtrie and K. M. Mullen, *New J. Chem.*, 2020, **44**, 11231–11236.
- 73 H. Wilson, S. Byrne, N. Bampos and K. M. Mullen, *Org. Biomol. Chem.*, 2013, **11**, 2105.
- 74 D. A. Leigh, V. Marcos, T. Nalbantoglu, I. J. Vitorica-Yrezabal, F. T. Yasar and X. Zhu, *J. Am. Chem. Soc.*, 2017, **139**, 7104–7109.
- 75 I. Neira, A. Blanco-Gómez, J. M. Quintela, C. Peinador and M. D. García, *Org. Lett.*, 2019, **21**, 8976–8980.
- 76 R. Scott Lokey and B. L. Iverson, *Nature*, 1995, **375**, 303–305.
- 77 S. Burattini, H. M. Colquhoun, J. D. Fox, D. Friedmann, B. W. Greenland, P. J. F. Harris, W. Hayes, M. E. Mackay and S. J. Rowan, *Chem. Commun.*, 2009, 6717–6719.
- 78 M. J. Gunter, N. Bampos, K. D. Johnstone and J. K. M. Sanders, *New J. Chem.*, 2001, **25**, 166–173.
- 79 M. Asakawa, P. R. Ashton, S. E. Boyd, C. L. Brown, R. E. Gillard, O. Kocian, F. M. Raymo, J. F. Stoddart, M. S. Tolley, A. J. P. White and D. J. Williams, *J. Org. Chem.*, 1997, **62**, 26–37.
- 80 C. G. Claessens and J. F. Stoddart, *J. Phys. Org. Chem.*, 1997, **10**, 254–272.
- 81 A. C. Fahrenbach, C. J. Bruns, D. Cao and J. F. Stoddart, *Acc. Chem. Res.*, 2012, **45**, 1581–1592.
- 82 V. Theodorou, K. Skobridis, A. G. Tzakos and V. Ragoussis, *Tetrahedron Lett.*, 2007, **48**, 8230–8233.
- 83 The hydrazone exchange equilibrium can be reached within a few days of reaction but is typically monitored for several weeks; see S. L. Roberts, R. L. E. Furlan, S. Otto and J. K. M. Sanders, *Org. Biomol. Chem.*, 2003, **1**, 1625–1633.
- 84 Unfortunately the corresponding dumbbell **16.2PF₆⁻** was unable to be purified by column chromatography.

- 85 P. A. Keifer, L. Baltusis, D. M. Rice, A. A. Tymiak and J. N. Shoolery, *J. Magn. Reson.*, 1996, **119**, 65–75.
- 86 K. M. Mullen, K. D. Johnstone, M. Webb, N. Bampos, J. K. M. Sanders and M. J. Gunter, *Org. Biomol. Chem.*, 2008, **6**, 278–286.
- 87 Red colouration of the resin beads arising from the donor-acceptor complex formation between the crown macrocycles and the naphthalene diimide threads was strongly indicative of attachment of rotaxane to the bead, as was also observed in the solution phase analogue **6**.
- 88 D. G. Hamilton, J. E. Davies, L. Prodi and J. K. M. Sanders, *Chem. – Eur. J.*, 1998, **4**, 608–620.
- 89 Y. Domoto, S. Sase and K. Goto, *Chem. – Eur. J.*, 2014, **20**, 15998–16005.